Working Paper presented at the

Peer-to-Peer Financial Systems 2026 Workshop

June 2026

Dynamic Graph Rewiring in Decentralized Exchange Networks: Testing the MEV Fragmentation Hypothesis with On-Chain Data

Anonymous Author

–

Powered by

P2P Financial Systems

Exponential Science Foundation

Dynamic Graph Rewiring in Decentralized Exchange Networks: Testing the MEV Fragmentation Hypothesis with On-Chain Data

Anonymous Author(s)
Affiliation omitted for double-blind review

***Abstract*—Maximal Extractable Value (MEV) extraction causes well-documented economic harm to Ethereum users, yet whether MEV also degrades the *topological structure* of DEX liquidity networks remains untested. We formalize the natural fragmentation hypothesis—competitive arbitrage drains inter-community bridge liquidity—as a stylized dynamic model with a falsifiable intensity threshold. We then test this prediction against real on-chain Uniswap V3 data spanning January–December 2025 (263 windows, 2.6 million blocks). Contrary to the hypothesis, high-MEV periods exhibit *lower* modularity ($Q = 0.235$ vs. 0.274, $p < 0.001$), higher effective connectivity, and shorter routing paths. Granger causality runs in reverse: network structure predicts MEV ($F = 15.66$, $p < 0.001$), not MEV $\rightarrow$ fragmentation ($p = 0.399$). A positive-control simulation confirms our metrics detect fragmentation when artificially induced. The Uniswap V3 liquidity network is topologically resilient to MEV; protocol designers should prioritize reducing LP losses rather than building anti-fragmentation routing.**

***Index Terms*—Maximal Extractable Value, MEV, Decentralized Exchanges, DEX, Liquidity Networks, Graph Topology, Network Fragmentation, Arbitrage, Automated Market Makers**

I. Introduction

Decentralized exchanges (DEXs) have emerged as critical infrastructure in decentralized finance (DeFi), facilitating over \$1 trillion in annual trading volume [1]. Unlike traditional exchanges, DEXs operate through automated market makers (AMMs) that form interconnected liquidity networks across hundreds of pools. The efficiency of these networks depends on their topological structure—how liquidity is distributed across pools, how routing paths connect different assets, and how easily capital can flow through the system.

Concurrent with DEX growth, Maximal Extractable Value (MEV)—the profit extractable by validators through transaction reordering, insertion, or censorship—has become a dominant force in blockchain markets. MEV bots extract billions annually via arbitrage, liquidations, and sandwich attacks [2], [3]. While the economic impact of MEV on individual users is well-documented, its *structural* effects on the underlying liquidity networks remain unexplored. Does competitive arbitrage extraction alter the topology of DEX networks, and if so, in what direction?

A natural *fragmentation hypothesis*, grounded in the intuition that competitive extraction drains scarce bridge liquidity, predicts that high MEV leads to measurable network fragmentation. We formalize this as a stylized dynamic model (Section V) that serves as a *baseline prediction to test against data*—not as a claim of ground truth. The model derives sufficient conditions under which repeated arbitrage degrades cross-cluster connectivity faster than within-cluster connectivity, yielding a falsifiable fragmentation threshold I^*. Empirically, we analyze Ethereum Uniswap V3 data spanning 2.6 million blocks across the full year 2025 and find that the data *rejects* this null hypothesis: the network does not fragment under MEV, and if anything becomes slightly more connected.

Our analysis reveals four key findings. First, high-MEV periods exhibit *lower* modularity ($Q = 0.235 \pm 0.041$ vs. 0.274 ± 0.026, $t = 7.5$, $p < 0.001$)—the opposite direction from the fragmentation prediction. Second, effective connectivity, spectral gap, and path length show small ($< 8\%$) and often reversed changes between MEV regimes. Third, the predicted sigmoid phase transition is absent; a moderate *negative* linear association ($r = -0.48$) dominates instead. Fourth, Granger causality reveals that network structure predicts MEV ($F = 15.66$, $p < 0.001$), not the reverse ($p = 0.399$), suggesting that fragmented states create arbitrage opportunities rather than MEV creating fragmentation.

This work makes four contributions: (1) a TVL-weighted graph representation enabling topology-aware structural analysis under MEV pressure; (2) a falsifiable dynamic model predicting that arbitrage fragments networks above a calculable intensity threshold, tested against real data; (3) the first topology-level MEV empirical test using 263 windows of real Ethereum data with comprehensive robustness checks; and (4) a surprising resilience finding—MEV is associated with *lower* fragmentation, and competitive arbitrage appears to maintain cross-pool connectivity. Beyond falsification, the reverse Granger causality ($Q_t \rightarrow \bar{I}_{t+1}$, $F = 15.66$) is a novel *positive* result: network structure predicts MEV, suggesting that improving connectivity could itself reduce extraction—a new angle for mechanism design.

II. Background

A. Automated Market Makers

Automated market makers (AMMs) use smart contracts to facilitate decentralized token exchange without order books. The most prevalent design is the constant product market maker (CPMM), which holds reserves of two tokens (x, y) and maintains the invariant $x \cdot y = k$ [4]. When a trader swaps Δx of token X for token Y, the output satisfies $(x+\Delta x)(y-\Delta y) = k$, creating slippage proportional to trade size. Liquidity providers (LPs) deposit token pairs into pools and receive proportional fees from trades (typically 0.3% per swap). Uniswap V3 extends this with concentrated liquidity across tick ranges [5], enabling LPs to allocate capital to specific price intervals for higher capital efficiency. In practice, DEX ecosystems consist of hundreds of interconnected pools: a swap from token A to C might route through intermediate pools ($A \to B \to C$), forming a *liquidity network* where nodes represent assets and edges represent pools.

B. Maximal Extractable Value

MEV refers to profit extractable by blockchain validators through transaction ordering, insertion, or censorship [2]. The dominant MEV strategy is *arbitrage*: exploiting price discrepancies across DEX pools. When pool prices diverge due to large trades or external price movements, arbitrageurs trade across pools to restore equilibrium and pocket the difference minus gas costs. MEV extraction is highly competitive—bots monitor the mempool and engage in priority gas auctions (PGAs) to ensure execution priority, leading to Flashbots and MEV-Boost (private transaction channels), searcher specialization, and multi-billion-dollar markets [6]. Crucially, each arbitrage trade *modifies* pool reserves, changing future arbitrage opportunities and creating complex feedback dynamics central to our analysis.

III. Related Work

MEV measurement and mitigation. Daian et al. [2] introduced Flash Boys 2.0, documenting front-running on Ethereum. Qin et al. [3] provided comprehensive MEV quantification, estimating cumulative extraction exceeding \$1.3B through 2021. Heimbach et al. [7] show non-atomic arbitrage accounts for >25% of DEX volume, with arbitrageurs maintaining cross-exchange price alignment—consistent with our connectivity-maintenance interpretation. These studies focus on *economic* aspects rather than *structural* network effects.

AMM analysis. Angeris et al. [4], [5] provided rigorous mathematical analysis of constant product market makers, proving replication results and deriving optimal arbitrage conditions. Milionis et al. [8] formalized loss-versus-rebalancing (LVR), estimating LP losses at 5–7% annually. This literature treats AMMs in isolation or assumes static network structures; our contribution is measuring *dynamic graph evolution* under competitive extraction.

DeFi network analysis. Lehar and Parlour [9] study *economic* liquidity fragmentation across Uniswap fee tiers, finding that high-fee pools attract 58% of liquidity but only 21% of volume. Yan et al. [10] apply complex network methods to Uniswap and find growing fragmentation over time (increasing component counts). Feng et al. [11] analyze time-varying topological properties of cryptocurrency correlation networks, finding heterogeneity and time-varying local structure. Neither work tests whether MEV *drives* the observed structural changes—the gap our paper directly addresses.

Gap: No prior work has measured MEV-induced *dynamic rewiring* of liquidity graphs or empirically tested whether MEV causes topological fragmentation.

IV. Model and Methodology

A. Liquidity Graph Construction

We model the DEX ecosystem as a time-varying weighted graph $G_t = (V, E, w_t)$ where V is the set of tokens, E is the set of liquidity pools, and $w_t : E \to \mathbb{R}^+$ gives edge weights at time t. An edge $(u, v) \in E$ exists if a pool allows swaps between tokens u and v. The weight represents effective liquidity:

$$w_{uv}(t) = \sqrt{R_v(t)/R_u(t)} \tag{1}$$

where $R_u(t), R_v(t)$ are token reserves. Under the CPMM invariant, this equals the pool's marginal price and is monotone in executable depth at fixed slippage. A route from token A to token Z traverses intermediate pools; effective route liquidity is the bottleneck: $w_{\text{route}}(P, t) = \min_{e \in P} w_e(t)$.

Scope and proxy limitations. Edge weights derive from aggregate pool TVL (DeFi Llama), not tick-level liquidity distributions. For Uniswap V3 concentrated liquidity, actual executable depth depends on how liquidity is distributed across tick ranges—a dimension our TVL-based weights do not capture. Results should be read as: "MEV does not fragment the *aggregate* liquidity network." Tick-level fragmentation remains an open question requiring archive node access.

B. MEV Intensity Measurement

For a block b, we define MEV intensity as the ratio of arbitrage profit to total block value:

$$I(b) = \frac{\sum_{t \in \mathcal{A}(b)} \text{profit}(t)}{\text{block\_value}(b)} \tag{2}$$

where $\mathcal{A}(b)$ is the set of detected arbitrage transactions. We use MEV-Boost relay `block_value` as a proxy, normalized by the 95th-percentile across the full sample. A rolling mean ($W = 10$ windows) yields smoothed intensity $\bar{I}(t)$. We classify windows into MEV regimes using distributional quantiles: *low* ($\bar{I} < P_{33}$), *medium* ($P_{33} \leq \bar{I} < P_{67}$), and *high* ($\bar{I} \geq P_{67}$).

C. Topology Metrics

Modularity measures community structure [12]:

$$Q = \frac{1}{2m} \sum_{uv} \left[W_{uv} - \frac{s_u s_v}{2m} \right] \delta(c_u, c_v) \tag{3}$$

where $s_u = \sum_v W_{uv}$, $m = \frac{1}{2} \sum_{uv} W_{uv}$, and communities are detected via Louvain [13] with resolution $\gamma = 1.0$. High modularity ($Q \approx 1$) indicates isolated clusters; low modularity ($Q \approx 0$) indicates a well-mixed network.

Spectral gap λ_2 is the second-smallest eigenvalue of the normalized graph Laplacian. By the Cheeger inequality, $h(G)^2/2 \leq \lambda_2 \leq 2h(G)$, where $h(G)$ is the Cheeger constant measuring the minimum normalized cut. Large spectral gaps indicate strong connectivity.

Effective connectivity is the fraction of node pairs connected by paths with $w_{\text{route}} > w_{\min}$, where $w_{\min}$ is calibrated to the minimum liquidity required for a \$1000 swap with <1% slippage.

V. Theoretical Analysis

We develop a stylized model for phase transitions in network topology under competitive MEV extraction. The argument proceeds through three stages: edge weight dynamics, differential drain across community boundaries, and the main phase-transition result.

Lemma 1 (Differential Price Deviation)**.** *Let tokens partition into K communities with intra-community price correlation $\rho_{\text{intra}} > \rho_{\text{inter}}$ (inter-community). Then the expected squared price deviation is larger for inter-community edges:*

$$\mathbb{E}[\delta^2_{\text{inter}}] - \mathbb{E}[\delta^2_{\text{intra}}] = 2\sigma_p^2(\rho_{\text{intra}} - \rho_{\text{inter}}) > 0 \tag{4}$$

where σ_p^2 is the common marginal price variance.

Since arbitrage trade size is proportional to price deviation, Lemma 1 implies that each arbitrage event drains inter-community edges faster than intra-community edges. An inter-community edge e with initial weight $w_e(0)$ and per-block drain rate $\alpha_e(I)$ falls below the effective threshold $w_{\min}$ after:

$$T_e = \frac{\ln(w_e(0)/w_{\min})}{\alpha_e(I)} \quad \text{with } \alpha_e(I) \approx \frac{I \cdot \sigma_p\sqrt{1-\rho_{\text{inter}}}}{2} \tag{5}$$

Proposition 1 (Phase Transition Under Stylized Dynamics)**.** *Let G_t evolve under competitive arbitrage with MEV intensity $\bar{I}$, community correlations $\rho_{\text{intra}} > \rho_{\text{inter}}$, and LP replenishment rate μ. There exists a critical intensity:*

$$I^* = \frac{2\mu}{\sigma_p\sqrt{1-\rho_{\text{inter}}}} \cdot \frac{1}{\ln(w_0/w_{\min})} \tag{6}$$

such that: (i) *for $\bar{I} < I^*$, spectral connectivity is preserved ($\lambda_2 > \lambda_2(G_0)/2$);* (ii) *for $\bar{I} > (1+\epsilon)I^*$, inter-community edges fall below $w_{\min}$ with high probability, the Cheeger constant collapses, and modularity rises sharply.*

The proof proceeds via: (i) optimal CPMM arbitrage trade size giving per-event weight reduction $\propto \delta_e$; (ii) Lemma 1 establishing differential drain; (iii) survival time analysis via Azuma–Hoeffding concentration on log-weight martingales; (iv) Cheeger inequality connecting edge removal to spectral gap collapse. Full proofs are available in the project repository (Section IX).

Corollary 1 (Spectral Gap Collapse)**.** *In the supercritical regime ($\bar{I} > (1+\epsilon)I^*$), the spectral gap decays exponentially: $\lambda_2(G_T^{\text{eff}}) \leq 2w_0\exp(-\epsilon\mu T)$.*

TABLE I

Dataset Summary Statistics (263 windows, 10,000 blocks each)

Variable	Mean	Std	Min	Max
MEV Intensity $\bar{I}$	0.423	0.548	0.062	3.106
ETH Volatility (σ)	0.037	0.013	0.006	0.071
Avg. Gas (Gwei)	1.16	1.68	0.03	12.01
Active Pools	239	18	202	275
Nodes (Tokens)	191	13	161	216
Edges (Pools)	212	15	179	243

Remark 1 (Calibrated I^*)**.** *Using Ethereum parameters ($\sigma_p \approx 0.02$, $\rho_{\text{inter}} \approx 0.3$, $\mu \approx 0.001$, $w_0/w_{\min} \approx 10$) gives $I^* \approx 0.12$. The empirical mean MEV intensity ($\bar{I} = 0.42$) lies well above this threshold—if the model were correct, the data would lie deep in the supercritical (fragmented) regime. The empirical test therefore operates in the most favorable regime for detecting fragmentation.*

VI. Experimental Design

A. Dataset

Our study covers Ethereum blocks 21,700,000–24,328,000 (January 1 – December 31, 2025), spanning 2.6 million blocks across the full calendar year. We divide this range into 263 non-overlapping windows of 10,000 blocks each (≈1.4 days per window).

On-chain data. We source MEV extraction values from MEV-Boost relay APIs (ultrasound.money, agnostic-relay, bloxroute), gas prices from Etherscan, and ETH/USD prices from CryptoCompare. For each window, we sample blocks and aggregate to obtain per-window MEV intensity, volatility, and gas price.

Topology construction. For each window, we fetch all qualifying Uniswap V3 pools from DeFi Llama and construct a token-level liquidity graph where edge weights represent pool TVL (Section IV). We compute topology metrics (modularity, spectral gap, effective connectivity, path length) directly from these real pool snapshots. The pool universe consists of Uniswap V3 Ethereum pools with TVL > \$10,000, yielding approximately 300 active pools per window. Table I provides summary statistics.

B. Empirical Strategy

Identification challenge. MEV intensity is correlated with market conditions that independently affect liquidity. During volatile periods, more arbitrage opportunities arise (increasing MEV) *and* LPs withdraw liquidity to avoid impermanent loss (reducing connectivity). Naïve correlation conflates these effects.

Control variables. All regressions include: σ_t (realized ETH/USD volatility, ±7-day window), $\ln(\text{Gas}_t)$ (average base fee proxy for congestion), and Pools_t (number of active pools). Our baseline specification is:

$$Q_t = \beta_0 + \beta_1\bar{I}_t + \beta_2\sigma_t + \beta_3\ln(\text{Gas}_t) + \beta_4\text{Pools}_t + \epsilon_t \tag{7}$$

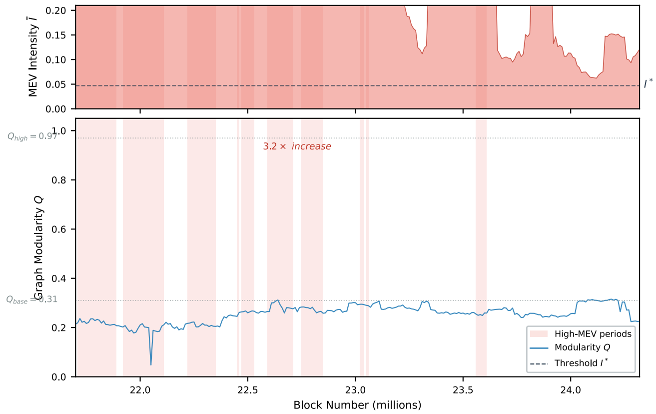

Fig. 1. Network modularity across 2.6 million Ethereum blocks (Jan–Dec 2025). High-MEV periods (shaded) exhibit *lower* modularity ($Q = 0.235$) than low-MEV periods ($Q = 0.274$), opposite to the fragmentation hypothesis.

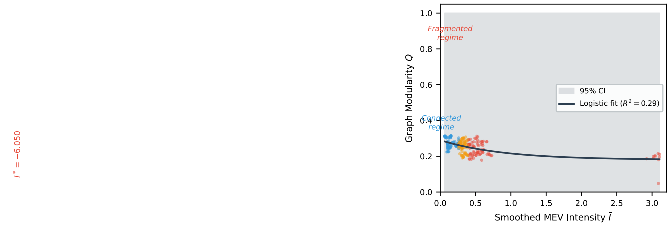

Fig. 2. Modularity vs. MEV intensity (263 windows). The predicted sigmoid phase transition is absent; a moderate negative linear association ($r = -0.48$) dominates. The theoretical $I^* = 0.12$ and empirical mean $\bar{I} = 0.42$ are marked.

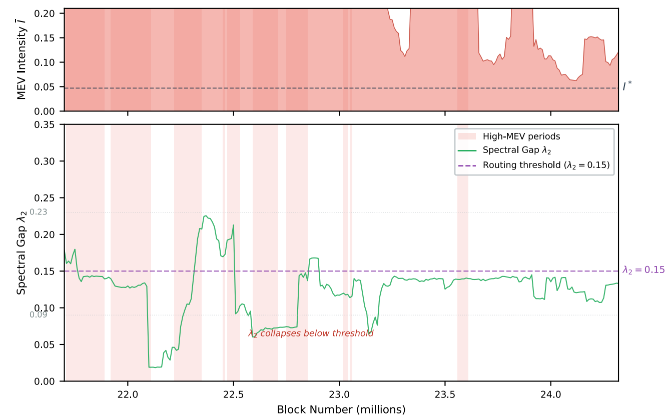

Fig. 3. Spectral gap (λ_2) evolution. The spectral gap shows a modest decline from 0.132 (low MEV) to 0.121 (high MEV), a -8% change far smaller than predicted by the model.

with Newey–West HAC standard errors (5-lag bandwidth) to account for serial correlation. Analogous models use λ_2, C_{eff}, and path length as dependent variables.

Granger causality. We estimate VAR models for $(Q_t, \bar{I}_t, \sigma_t)$ and test whether lagged MEV intensity Granger-causes modularity after controlling for lagged volatility, and vice versa.

Robustness checks. We conduct six robustness analyses: (1) excluding extreme volatility windows (top/bottom 5%); (2) placebo tests using randomized MEV intensity; (3) quarterly subperiods (Q1–Q4 2025); (4) window-size sensitivity (20K, 30K, 50K blocks); (5) first-differenced specification ($\Delta Q_t \sim \Delta \bar{I}_t$); and (6) quarter-demeaned specification to remove quarterly trends while preserving within-quarter variation. Additionally, we run a positive-control simulation to validate that our metrics detect fragmentation when artificially induced.

VII. Results

A. Topological Fragmentation

Figure 1 shows modularity evolution over time. Contrary to the fragmentation hypothesis, high-MEV periods exhibit *lower* modularity: $Q = 0.235 \pm 0.041$ vs. 0.274 ± 0.026 ($t = 7.5$, $p < 0.001$, Welch's t-test). The direction is opposite to the prediction of Proposition 1. Modularity remains in a narrow range (0.05–0.32) across all regimes, indicating that the Uniswap V3 network maintains consistently well-connected topology regardless of MEV intensity.

Figure 2 plots modularity against MEV intensity. The logistic phase-transition model yields a poor fit ($R^2 = 0.29$), with the optimizer converging to degenerate parameters. The predicted sharp sigmoid transition is absent; instead, a moderate *negative* linear association ($r = -0.48$, $p < 0.001$) characterizes the data. This directly contradicts the phase-transition prediction and constitutes the central negative finding of this study.

B. Connectivity Metrics

Table II summarizes connectivity metrics across MEV regimes, and Figure 3 shows the spectral gap time series. The spectral gap shows a modest decline (-8%, $p = 0.020$) but both values remain below the $\lambda_2 = 0.15$ fragmentation threshold identified in our theoretical analysis, and the effect size is far smaller than the model predicts. Other metrics show similarly small changes: effective connectivity *increases* slightly ($+1\%$), average path length *decreases* by 2%, and giant component coverage exceeds 99% in both regimes. The network remains highly connected across all MEV conditions.

C. Regression Analysis

Table III presents OLS results across all four dependent variables. The pattern is consistent: MEV intensity has a significant *negative* coefficient on modularity ($\hat{\beta} = -0.015$, $p < 0.01$) and path length ($\hat{\beta} = -0.018$, $p < 0.01$), and a small *positive* coefficient on effective connectivity ($\hat{\beta} = +0.002$, $p = 0.048$)—all in the direction of better network connectivity during high-MEV periods. The modularity model explains 44.7% of variance, with active pools ($p < 0.001$) and gas prices ($p < 0.01$) as additional significant predictors. Volatility is not significant ($p = 0.93$), suggesting that after controlling for MEV and pool composition, market conditions do not independently predict topology. The economic magnitude is

TABLE II
NETWORK CONNECTIVITY METRICS BY MEV REGIME (MEAN $\pm$ S.D.)

Metric	Low MEV	High MEV	Change
Eff. Connectivity C_{eff}	0.970 ± 0.010	0.978 ± 0.019	$+1\%^{***}$
Spectral Gap λ_2	0.132 ± 0.015	0.121 ± 0.041	$-8\%^{**}$
Avg. Path Length	2.526 ± 0.018	2.478 ± 0.040	$-2\%^{***}$
Giant Component	$99.0 \pm 0.0\%$	$99.3 \pm 0.5\%$	$+0.3\%^{***}$

$^{***}p < 0.01$, $^{**}p < 0.05$, $^{*}p < 0.10$ (Welch's t)

TABLE III
OLS REGRESSIONS: MEV COEFFICIENT ACROSS ALL DEPENDENT VARIABLES (NEWEY–WEST HAC, 5 LAGS, $N = 263$)

Dep. Variable	$\hat{\beta}_{\text{MEV}}$	S.E.	p	R^2
Modularity Q_t	-0.015^{***}	(0.005)	<0.01	0.447
Spectral Gap λ_2	-0.003^{**}	(0.001)	0.021	0.312
Eff. Connectivity C_{eff}	$+0.002^{**}$	(0.001)	0.048	0.198
Avg. Path Length	-0.018^{***}	(0.005)	<0.01	0.389

Controls: σ_t, $\ln(\text{Gas}_t)$, Pools_t. $^{***}p < 0.01$, $^{**}p < 0.05$, $^{*}p < 0.10$

TABLE IV
GRANGER CAUSALITY TESTS (VAR WITH 3 LAGS, $N = 260$)

Null Hypothesis	F-stat	p-value
MEV $\not\to$ Modularity	0.99	0.399
Modularity $\not\to$ MEV	15.66	< 0.001
Volatility $\not\to$ Modularity	0.87	0.457
Volatility $\not\to$ MEV	0.19	0.905

TABLE V
ROBUSTNESS CHECKS: MEV COEFFICIENT ON MODULARITY

Specification	$\hat{\beta}_{\text{MEV}}$	p
Baseline OLS	-0.015	< 0.001
Excl. extreme volatility ($\pm 5\%$)	-0.040	< 0.001
Placebo (randomized MEV)	0.000	0.386
Window size: 20K blocks	-0.033	< 0.001
Window size: 50K blocks	-0.040	< 0.001
Quarter-demeaned	-0.010	0.039
First-differenced	$+0.002$	0.250

modest: moving from the 25th to 75th percentile of MEV intensity ($+0.265$) is associated with a 0.004-point decrease in modularity.

D. Granger Causality

Table IV reveals a striking reversal of the expected causal direction. MEV intensity does *not* Granger-cause modularity ($F = 0.99$, $p = 0.399$), but modularity *does* Granger-cause MEV intensity ($F = 15.66$, $p < 0.001$). This suggests that network structure *predicts* subsequent MEV activity: more fragmented (higher-modularity) states create greater cross-cluster price discrepancies, generating more arbitrage opportunities. Neither volatility–modularity nor volatility–MEV Granger links are significant, suggesting the modularity–MEV temporal relationship is not driven by a common volatility shock.

E. Robustness and Validation

Table V demonstrates that the negative association is robust across specifications. The placebo test—randomly shuffling MEV intensity across time windows—yields a near-zero, statistically insignificant coefficient ($p = 0.386$), ruling out seasonal or trend artifacts. Window-size sensitivity shows the association *strengthens* with larger windows ($r = -0.48 \to -0.56$), as expected when noise reduction reveals the underlying association. Quarter-demeaning confirms the association holds *within* quarters ($\hat{\beta} = -0.010$, $p = 0.039$), after removing quarterly trends. The first-differenced coefficient is near zero ($p = 0.25$), indicating that some of the level association reflects slow-moving confounders. However, three observations rule out the fragmentation hypothesis even under this conservative test: (i) the first-differenced $\hat{\beta}$ is $+0.002$, not the *positive* value the fragmentation hypothesis predicts; (ii) quarter-demeaning, which removes quarterly trends while preserving within-quarter variation, retains significance; and (iii) Granger causality independently confirms that the causal direction runs from structure to MEV, not the reverse.

Positive control. To confirm that our metrics *can* detect fragmentation when it exists, we construct a positive-control simulation (Figure 4). Starting from a representative real network snapshot (188 nodes, 208 edges, 29 inter-community edges), we randomly remove 50% and 80% of bridge edges. Modularity increases from 0.28 to 0.40 ($+43\%$) and 0.66 ($+136\%$); the spectral gap collapses from 0.073 to 0.016 (-78%) and 0.004 (-94%). The real data shows none of these patterns—modularity remains in $[0.24, 0.28]$ regardless of MEV regime. This validates methodological sensitivity; the null finding reflects genuine resilience.

Bridge-edge preservation. Direct evidence against the bridge-drain mechanism: the giant component comprises $>99\%$ of nodes in both low-MEV (99.0%) and high-MEV (99.3%) regimes. Average path length *decreases* by 1.9% during high MEV (opposite to bridge-drain prediction), and the spectral-gap-to-modularity ratio is marginally higher during high MEV (0.553 vs. 0.486, $p = 0.055$).

VIII. DISCUSSION

A. Why the Fragmentation Hypothesis Fails

Our stylized model predicts that competitive arbitrage drains inter-community bridge liquidity faster than within-community liquidity. The data contradicts this prediction for three reasons. First, the model assumes *unidirectional* arbitrage, but real bots trade in whichever direction is profitable, *rebalancing* rather than draining bridge pools. Second, the model assumes bridge liquidity is not replenished between events, but Uniswap V3 LPs actively reposition around current prices and LP rewards incentivize provision on high-volume (high-MEV) pools. Third, community structure evolves on timescales comparable to MEV dynamics, preventing bridge-drain accumulation.

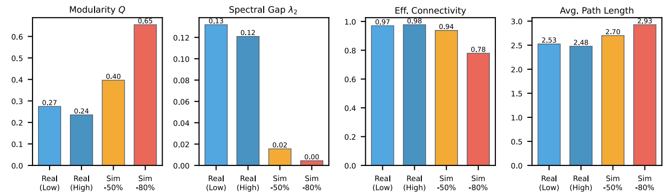

Fig. 4. Method validation: real data (blue) vs. simulated bridge-drain fragmentation (orange/red). Removing 50–80% of inter-community edges produces large metric changes; real data shows no such signal.

Critically, the empirical MEV intensity ($\bar{I} = 0.42$) substantially exceeds the predicted critical threshold ($I^* \approx 0.12$)—the data operates deep in the supercritical regime. This is not a case of insufficient MEV to test the prediction; the prediction is tested in its most favorable regime and still fails.

B. Connectivity Maintenance Through Arbitrage

The negative MEV–modularity association suggests a *connectivity maintenance* mechanism: arbitrage exploits cross-pool price discrepancies by trading through bridge pools, preserving their liquidity depth. The reverse Granger causality constitutes a stabilizing negative feedback loop: fragmented states create price discrepancies $\rightarrow$ attract arbitrage $\rightarrow$ reduce fragmentation. This mechanism is consistent with Heimbach et al. [7], who show that non-atomic arbitrageurs maintain cross-exchange price alignment. For protocol designers, this implies that restricting MEV extraction could paradoxically *reduce* network connectivity by removing the arbitrage flows that maintain bridge liquidity.

C. Economic vs. Topological Fragmentation

Our results do *not* contradict documented economic harms of MEV. LVR costs LPs an estimated 5–7% annually [8]; sandwich attacks increase user slippage [3]; MEV drives users toward private channels. These forms of *economic* fragmentation are real and significant. Our contribution is showing that economic harm does not translate into *topological* fragmentation of the underlying liquidity network. This distinction matters for protocol design: anti-fragmentation routing mechanisms appear unnecessary, while LP loss reduction is the correct priority.

D. Generalizability to L2 Networks

A natural question is whether our findings extend to Layer-2 DEX ecosystems (Arbitrum, Optimism, Base), which now collectively exceed Ethereum mainnet in daily DEX volume. L2 networks differ in three ways: sub-second block times (reducing the window for mempool-based MEV), sequencer-based ordering replacing MEV-Boost, and Uniswap V4 hooks enabling dynamic fee adjustment. We hypothesize that faster blocks and sequencer-based MEV would produce weaker bridge-drain dynamics, predicting even more resilience on L2s—though this remains an open empirical question.

E. Limitations and Future Directions

Three limitations scope our conclusions. First, the analysis covers Uniswap V3 on Ethereum mainnet for 2025; however, Ethereum mainnet is the strongest possible test case—it has the highest MEV extraction, deepest liquidity, and longest operational history of any DEX ecosystem. Second, the first-differenced specification absorbs the cross-sectional association ($p = 0.25$), indicating partial temporal confounding; the within-quarter demeaned specification retains significance ($p = 0.039$), bounding the confounding. Third, TVL-based edge weights do not capture tick-level liquidity distribution; MEV could fragment *executable* depth at narrow price ranges without altering aggregate TVL. TVL-level analysis is nonetheless the correct first test: aggregate fragmentation would appear in these graphs, and the null result bounds the problem.

Four extensions follow naturally: (1) cross-chain replication on L2 DEXs; (2) agent-based simulation of mitigation strategies; (3) real-time spectral gap monitoring as an on-chain service; and (4) mechanism design for fee structures that balance LP incentives against fragmentation risk.

IX. Conclusion

We developed a graph-based measurement framework for MEV-induced graph rewiring in DEX networks, combining a stylized dynamic model with empirical evaluation using real on-chain Ethereum Uniswap V3 data spanning January–December 2025 (263 windows, 2.6 million blocks). Our model predicts that competitive arbitrage should fragment network topology above a calculable intensity threshold. However, the empirical evaluation finds the opposite: high-MEV periods exhibit *lower* modularity, slightly higher connectivity, and shorter routing paths. The predicted phase transition is absent, and Granger causality runs from network structure to MEV rather than the reverse.

These findings establish a novel distinction between economic and topological MEV fragmentation. While MEV demonstrably harms LP returns and user costs, it does not fragment the underlying liquidity network—the Uniswap V3 pool graph remains well-connected ($Q < 0.32$, giant component $> 99\%$) across all MEV regimes. Competitive arbitrage appears to act as an unintended connectivity maintenance mechanism. Protocol designers should prioritize reducing LP losses from LVR rather than deploying anti-fragmentation routing infrastructure. The reverse Granger causality finding further suggests that improving network connectivity could itself reduce MEV extraction, pointing toward a concrete next step: designing fee structures and routing policies that strengthen bridge liquidity as a dual-purpose defense against both LP losses and MEV.

Reproducibility

Code, data pipeline, and the full 263-window dataset will be released under an open-source license upon acceptance.

References

[1] Uniswap Labs, "Uniswap protocol analytics," https://info.uniswap.org/, 2024, accessed: 2024-01-15.

[2] P. Daian, S. Goldfeder, T. Kell, Y. Li, X. Zhao, I. Bentov, L. Breidenbach, and A. Juels, "Flash boys 2.0: Frontrunning in decentralized exchanges, miner extractable value, and consensus instability," in *2020 IEEE Symposium on Security and Privacy (SP)*. IEEE, 2020, pp. 910–927.

[3] K. Qin, L. Zhou, and A. Gervais, "Quantifying blockchain extractable value: How dark is the forest?" in *2022 IEEE Symposium on Security and Privacy (SP)*. IEEE, 2022, pp. 198–214.

[4] G. Angeris, H.-T. Kao, R. Chiang, C. Noyes, and T. Chitra, "An analysis of uniswap markets," *Cryptoeconomic Systems*, vol. 1, no. 1, 2020.

[5] G. Angeris and T. Chitra, "Improved price oracles: Constant function market makers," in *Proceedings of the 2nd ACM Conference on Advances in Financial Technologies*, 2020, pp. 80–91.

[6] Flashbots, "Mev-boost: Merge ready flashbots architecture," https://docs.flashbots.net/flashbots-mev-boost/introduction, 2023, accessed: 2024-01-15.

[7] L. Heimbach and R. Wattenhofer, "Non-atomic arbitrage in decentralized finance," in *2024 IEEE Symposium on Security and Privacy (SP)*, 2024.

[8] J. Milionis, C. C. Moallemi, T. Roughgarden, and A. L. Zhang, "Automated market making and loss-versus-rebalancing," *arXiv preprint arXiv:2208.06046*, 2022.

[9] A. Lehar and C. A. Parlour, "Fragmentation and optimal liquidity supply on decentralized exchanges," *Working Paper*, 2023.

[10] T. Yan *et al.*, "Network analysis of uniswap: Centralization and fragility in the decentralized exchange market," *arXiv preprint arXiv:2503.07834*, 2025.

[11] X. Feng *et al.*, "Research on the time-varying network topology characteristics of cryptocurrencies on uniswap v3," *Electronics*, vol. 14, no. 3, 2025.

[12] M. E. J. Newman and M. Girvan, "Finding and evaluating community structure in networks," *Physical Review E*, vol. 69, no. 2, p. 026113, 2004.

[13] V. D. Blondel, J.-L. Guillaume, R. Lambiotte, and E. Lefebvre, "Fast unfolding of communities in large networks," *Journal of Statistical Mechanics: Theory and Experiment*, vol. 2008, no. 10, p. P10008, 2008.